Numerical study of hydraulic jumps on corrugated beds using turbulence models

A. ABBASPOUR, D. FARSADIZADEH,
A. HOSSEINADEH DALIR and A. A. SADRADDINI
Water Engineering Department, University of Tabriz,5166616471, Tabriz-IRAN.
e-mail: akabbaspour@yahoo.com

Abstract

Hydraulic jumps have been used for dissipation of kinetic energy downstream of hydraulic structures, such as spillways, chutes, and gates. It was found that if jumps were made to occur on corrugated beds, tail water and length of jumps reduced significantly. During the formation of the hydraulic jump on a corrugated bed, the flow is turbulent water and air mixing together. In the present study, 2-dimensional numerical simulation of hydraulic jump on a corrugated bed was evaluated using both standard k-ε and RNG k-ε models. The free surface was determined using the VOF method. The results showed that k-ε turbulent model and VOF method for predicting the water surface in the jump on a corrugated bed were suitable and the relative error of predicted water surface profiles and measured value were within a range of 1%-8.6%. The study of the axial velocity profiles at different sections in the jump found that velocity profiles in different experiments were similar and there was a good agreement between modeled and measured results. The effects of corrugations (t, s) on the basic characteristics of jump, such as free surface location, velocity, and shear stress distribution, were studied for a different range of Froude number.

Key Words: Hydraulic jump, corrugated bed, Navier-Stokes equations, volume of fluid (VOF), k-ε turbulence models.

Introduction

Hydraulic jump in a horizontal channel with a smooth bed has been studied extensively by many researchers (Vischer and Hager, 1995). Recently, some investigations have been carried out on rough and corrugated beds. However, the main concern with jumps on rough and corrugated beds is that the roughness elements and crest of corrugations might be subjected to cavitations and erosion thereby may damage the structure itself. Previous research conducted by Ead et al. (2000) showed that if the crests of corrugations are placed at the level of upstream bed carrying the supercritical flow, the corrugations would not protrude into the flow, hence prevent cavitations in the basin. Furthermore, they also reported that, in culvert with corrugated bed, Reynolds shear stresses are produced so the velocity field above the corrugations is reduced.

Ead and Rajaratnam (2002) studied hydraulic jumps on a corrugated bed experimentally in the range of Froude numbers from 4 to 10. Three values of the relative roughness t/y_1 (t is the height of corrugations and y_1

is the initial depth of flow) 0.50, 0.43, and 0.25 were studied. Tokyay (2005) investigated the effect of channel bed corrugations on a hydraulic jump experimentally. In the experiments 2 values of wave steepness, 0.20 and 0.26, were used and the range of Froude numbers was from 5 to 12. The results showed that many factors, such as initial depth of flow, supercritical Froude number, height and wave length of corrugations t, s were effective on the characteristics of the hydraulic jump.

Study of hydraulic jump on corrugated beds by analytical methods is tedious not only because of boundary layer problems but also due to complexity of turbulent flow and diffusion process involved between walls, bed, and rolling water surface. Hydraulic jump is a 2-phase turbulent flow and simulation of it by using turbulence models and VOF (volume-of-fluid) method can led to accurate results.

Gharangik and Chaudhry (1991) investigated a hydraulic jump by a numerical model. They applied the Boussinesq equations to simulate both the sub and supercritical flows and a hydraulic jump in a rectangular channel having a small bed slope. The numerical study of hydraulic jump on a smooth bed has also been carried out by Zhao and Misra (2004). The governing equations are the continuity and momentum for incompressible flow and based on the 2-dimensional k-ε turbulence model. They used the VOF and the scale turbulence model to predict water surface location and horizontal velocity. Sarker and Rhodes (2002) studied hydraulic jump on a smooth bed by physical and numerical methods. They used the RNG k-ε turbulence model in combination with the volume of fluid (VOF) method for free surface modeling. There was a good agreement between the 2-dimensional CFD solution and the physical measurements. Gonzalez and Bombardelli (2005) simulated a hydraulic jump on a smooth bed using k-ε turbulence and Large Eddy Simulation (LES) models. The simulated results were compared with observations of mean flow and turbulence in hydraulic jumps by Liu et al. (2004).

The objective of this research was to investigate the numerical model of hydraulic jump on a corrugated bed using standard and RNG k-ε turbulence models. This study was carried out with a CFD program, which uses the finite-volume method to solve 2D Reynolds-averaged Navier Stokes (RANS) equations. In this program, the free surface location is computed using the VOF (volume-of-fluid) method.

Materials and Methods

Governing equations

The governing equations are unsteady incompressible 2-dimensional continuity and Reynolds-averaged Navier-Stokes equations for liquid and air (Liu et al., 2002).

$$\frac{\partial \rho}{\partial t} + \frac{\partial}{\partial x_i}(\rho u_i) = 0 \tag{1}$$

$$\frac{\partial}{\partial t}(\rho u_j) + \frac{\partial}{\partial x_i}(\rho u_i u_j) = -\frac{\partial P}{\partial x_j} + \frac{\partial}{\partial x_i}(\mu + \mu_t)\left(\frac{\partial u_i}{\partial x_j} + \frac{\partial u_j}{\partial x_i}\right) + \rho g_j \tag{2}$$

$$\rho = \alpha_A \rho_A + \alpha_w \rho_w \tag{3}$$

$$\mu = \alpha_A \mu_A + \alpha_w \mu_w \tag{4}$$

where u_i is the velocity components, α_A and α_w are the volume fraction of air and water, ρ_A, ρ_w, and ρ are the density of air, water, and mixture respectively; P is the pressure; g is the acceleration due to gravity. The

parameters of μ, μ_A,μ_w, and μ_t are the viscosity of mixture, air, water, and the eddy viscosity, respectively. The turbulent viscosity, μ_t, is computed by combining k and ε as follows:

$$\mu_t = \rho C_\mu \frac{k^2}{\varepsilon} \qquad (5)$$

where $C_\mu = 0.09$ is a constant

Numerical model

In the present research, hydraulic jump on a corrugated bed was numerically studied for different Froude numbers using the k-ε models and the 2-phase flow theory.

Volume of fluid (VOF) The water surface location was determined with the volume of fluid (VOF) method. The VOF method uses a function F(x, y, t) to assign the free surface. The function F is obtained from the following equation

$$\frac{\partial F}{\partial t} + u_j \frac{\partial F}{\partial x_j} = 0 \qquad (6)$$

A unit value of F corresponds to a cell full of fluid, while a zero value indicates that the cell contains no fluid. Cells with F values between 0 and 1 contain a free surface. The function F can be solved with different methods. In this study a geometric reconstruction method was used. The geometric reconstruction scheme represents the interface between fluids using a piecewise-linear approach. This scheme is the most accurate one and is applicable for general unstructured meshes. In Figure 1 the interface between 2 fluids are represented for actual and the geometric reconstruction scheme.

Turbulence models In this study the hydraulic jump was modeled using 2-equation turbulence models including standard k-ε and RNG k-ε.

| (a) | (b) |
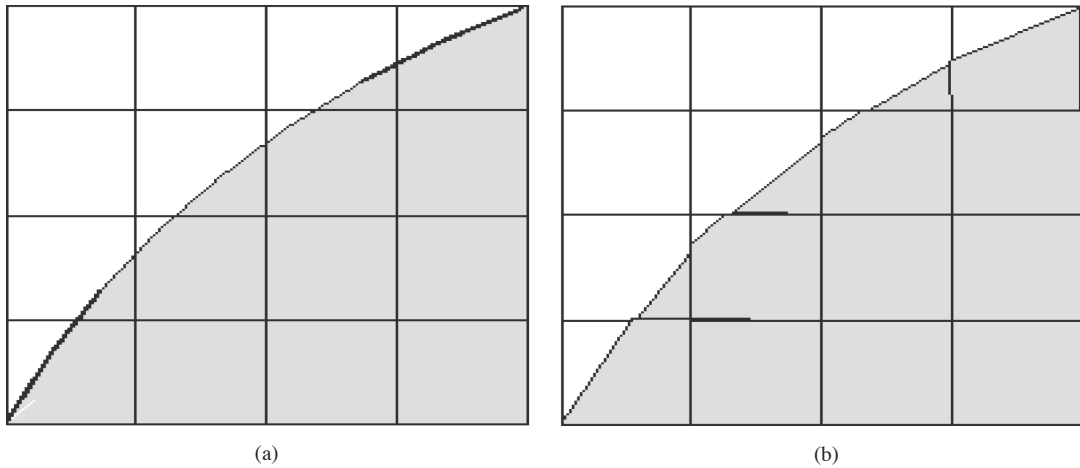
Figure 1. Interface Calculations; (a) actual interface shape; (b) the geometric reconstruction scheme.

Standard k-ε model Standard k-ε model is given by the following equations:

$$\rho u_i \frac{\partial k}{\partial x_i} = \mu_t \left(\frac{\partial u_j}{\partial x_i} + \frac{\partial u_i}{\partial x_j} \right) \frac{\partial u_j}{\partial x_i} + \frac{\partial}{\partial x_i} \left\{ (\mu_t/\sigma_k) \frac{\partial k}{\partial x_i} \right\} - \rho \varepsilon \qquad (7)$$

$$\rho u_i \frac{\partial \varepsilon}{\partial x_i} = C_{1\varepsilon} \left(\frac{\varepsilon}{k} \right) \mu_t \left(\frac{\partial u_j}{\partial x_i} + \frac{\partial u_i}{\partial x_j} \right) \frac{\partial u_j}{\partial x_i} + \frac{\partial}{\partial x_i} \left\{ (\mu_t/\sigma_\varepsilon) \frac{\partial \varepsilon}{\partial x_i} \right\} - C_{2\varepsilon}\rho \left(\frac{\varepsilon^2}{k} \right) \tag{8}$$

where k is turbulent kinetic energy and ε is dissipation rate. $\sigma_k = 1$ and $\sigma_\varepsilon = 1.3$ are the turbulent Prandtl numbers for k and ε, respectively. $C_{1\varepsilon} = 1.44$ and $C_{2\varepsilon} = 1.92$ are empirical constants.

RNG k-ε model The equations of RNG *k-ε* model are as following (Papageorgakis and Assanis, 1999):

$$\rho u_i \frac{\partial k}{\partial x_i} = \mu_t S^2 + \frac{\partial}{\partial x_i} \left(\alpha_k \mu_{eff} \frac{\partial k}{\partial x_i} \right) - \rho \varepsilon \tag{9}$$

$$\rho u_i \frac{\partial \varepsilon}{\partial x_i} = C_{1\varepsilon} \left(\frac{\varepsilon}{k} \right) \mu_t S^2 + \frac{\partial}{\partial x_i} \left(\alpha_\varepsilon \mu_{eff} \frac{\partial \varepsilon}{\partial x_i} \right) - C_{2\varepsilon}\rho \left(\frac{\varepsilon^2}{k} \right) - R \tag{10}$$

The term R is modeled as

$$R \equiv \frac{C_\mu \rho \eta^3 (1 - \eta/\eta_0)}{1 + \beta \eta^3} \frac{\varepsilon^2}{k} \tag{11}$$

$$\eta \equiv \frac{Sk}{\varepsilon} \tag{12}$$

$$S \equiv \sqrt{2S_{ij}S_{ij}}, S_{ij} \equiv \frac{1}{2} \left(\frac{\partial u_j}{\partial x_i} + \frac{\partial u_i}{\partial x_j} \right) \tag{13}$$

where $\alpha_k = \alpha_\varepsilon = 1.39$, $C_{1\varepsilon} = 1.42$, $C_{2\varepsilon} = 1.68$, $\eta_0 = 4.38$, and $\beta = 0.012$ are model constants. R and S are additional terms related to the mean rate of strain and turbulence quantities.

Model geometry and boundary conditions To analyze the hydraulic jump on a corrugated bed, the model geometry was generated and the unstructured grids were created. Considering small height of corrugations, the grids size near the corrugated bed was in the range of 5-9 mm, and for the rest of computational region, it was in the range of 10-22 mm. The view sketch of the initial regions and boundary conditions in the jump on the corrugated bed are shown in Figure 2.

The basic procedure is to define primary phase water and a secondary phase air as shown in Figure 2. As shown in Figure 2, the inlets were defined as the water flow (AB) and air flow (BC) into the domain. The boundary conditions also were defined as wall boundary condition (channel bed and gates), streamwise velocity or hydrostatic pressure inlets (AB), hydrostatic pressure inlet (BC), and outlet (DE) equal to zero. The values of the velocity and the turbulence parameters, i.e., the turbulent kinetic energy (k) and the dissipation (ε), were obtained from experimental data. To calculate the effect of the wall on the flow, empirical wall functions, known as standard equilibrium, were used. The time-dependent solution procedure was given an initial condition in which all of the cells upstream of the gate and up to velocity inlets level were patched as water filled; F =1.

Experimental procedure

The experiments were conducted in a metal-glass flume of rectangular cross section. The flume has the dimensions of 0.25 m width, 0.5 m depth, and 10 m length with a slope of 0.002. The flume is equipped with a sluice gate at the entrance and discharge was measured by a triangular weir placed at the end of it.
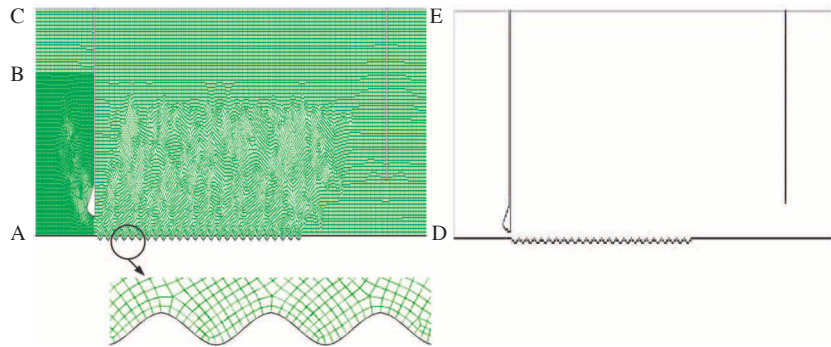
Figure 2. Boundary conditions and initial air and water flow regions.

The corrugated polyethylene sheets with sinusoidal corrugations of wave length s and height t were installed in the flume perpendicular to the flow direction. The crests of corrugations were at the level of upstream bed carrying the supercritical flow, hence acting as a depression and minimizing the intensity of cavitations. The supercritical approach flow was produced using a sluice gate. The tailwater depth is controlled by an adjustable gate at the end of the channel in such a way that the jumps are formed at the beginning of the corrugated bed. The water depths of the jump were measured using ultrasonic sensors at several sections in the flume and the data were saved on a computer and processed by VisiDAQ soft. The water surface profiles of the jumps on corrugated beds were measured at the centerline of the flume with a point gauge to an accuracy of ± 0.1 mm. The velocity profiles were also measured above the crest of corrugations at different sections with a micro propeller velocity meter to an accuracy of ± 0.1 cm/s. Supercritical depth y_1, tailwater depth y_2, and the length of the jump L_j, in the experiments D, E, F, G, H, and I were recorded and are presented in Table 1.

Table 1. Primary detail of the experiments.

| EXP.	sheet	t	s	q (m²/s)	u_1 (m/s)	y_1 (mm)	Fr_1	Re	y_2 (m)	L_j (m)
A_1	I	13	68	0.063	2.5	25.4	5	63500	0.128	0.48
A_2	I	13	68	0.089	3.49	25.4	7	88646	0.188	0.75
B_1	I	13	68	0.143	2.82	50.8	4	143256	0.21	0.88
B_2	I	13	68	0.207	4.07	50.8	5.8	206756	0.31	1.29
C_1	II	22	68	0.143	2.82	50.8	4	143256	0.21	0.82
C_2	II	22	68	0.207	4.07	50.8	5.8	206756	0.31	1.29
D	III	15	40	0.114	3.45	33	6.1	113850	0.22	0.75
E	IV	20	40	0.076	3.62	21.0	8	75970	0.178	0.7
F	V	25	40	0.098	3.15	31	5.7	97578	0.22	0.73
G	VI	20	70	0.114	3.36	34	5.8	114400	0.218	0.70
H	VII	25	70	0.071	3.29	21.5	7.2	70735	0.165	0.64
I	VIII	35	70	0.112	2.88	39	4.7	112320	0.215	0.68

In this study the measurements of Ead and Rajaratnam (2002) were also utilized. Its experimental set-up consists of a horizontal rectangular flume with plexiglas sidewalls, with 0.446 m width, 0.60 m depth, and 7.6 m length. Water entered the flume from underneath a vertical sluice gate produces a hydraulic jump next to the gate opening. Velocity profiles were measured at several vertical sections inside the jumps, in the center plane of the flume. The primary details of these tests are shown in Table 1 under the title of Experiments as A1, A2, B1, B2, C1, and C2.

Results and Discussion

Standard and RNG turbulent models were used to simulate the hydraulic jump on corrugated bed and the characteristics of jump, such as water surface profile, length of the jump, velocity profile in different sections, and bed shear stress were evaluated.

Water surface profile

The free surfaces obtained by the volume of fluid (VOF) method are shown in Figures 3 and 4. Simulated water surface profiles agreed well with the measured values. The mean relative error of water surface profiles between simulated and experimental values is about 1%-8.6%.
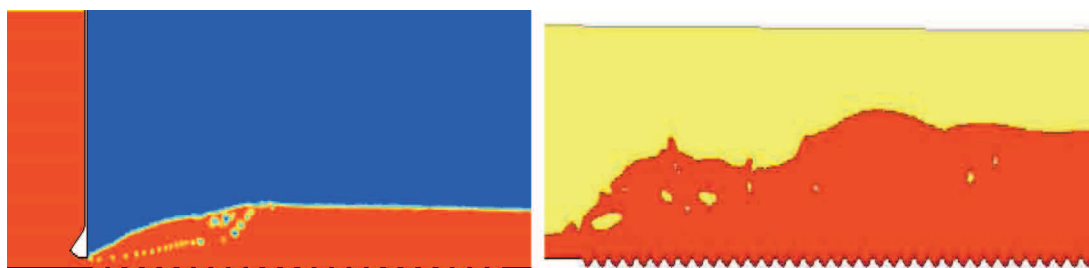
Figure 3. Simulation of water surface profiles using the VOF method for experiments A_2 and D.

In Figure 5 normalized water surface profiles, which were obtained by standard and RNG turbulent models, are shown. The numerical model values for mean curve of normalized water surface profiles agreed well with the experimental data.

Hydraulic jump length

The length of jump L_j can be obtained from the water surface profiles (Figure 4). The estimated values for the jump length are in good agreement with the measured values for the tests A_2, B_1, B_2, C_1, D, E, F, H, and I; however, there are a little difference between modeled and measured values for experiments A_1, C_2, and G. It may be due to the use of pressure outlet boundary after the gate, and to solve this problem, it is better to use a smaller computational region with defined pressure or velocity boundary before gate. The mean relative error of the length of jump between simulated and experimental values is about 1%-12%.

Velocity profiles

In Figure 6 normalized modeled and measured values of velocity profiles in the different sections of jumps are shown. In order to compare similarity of velocity profiles in the different sections of jumps, the maximum velocity u_m and the length scale b was determined. The length scale b is the value of y at which u $=0.5u_m$ and (du/dy) <0. Figure 6 shows that the velocity profiles are similar for experiments B_2, C_2 D, and G. A good agreement was found between numerical and experimental results.
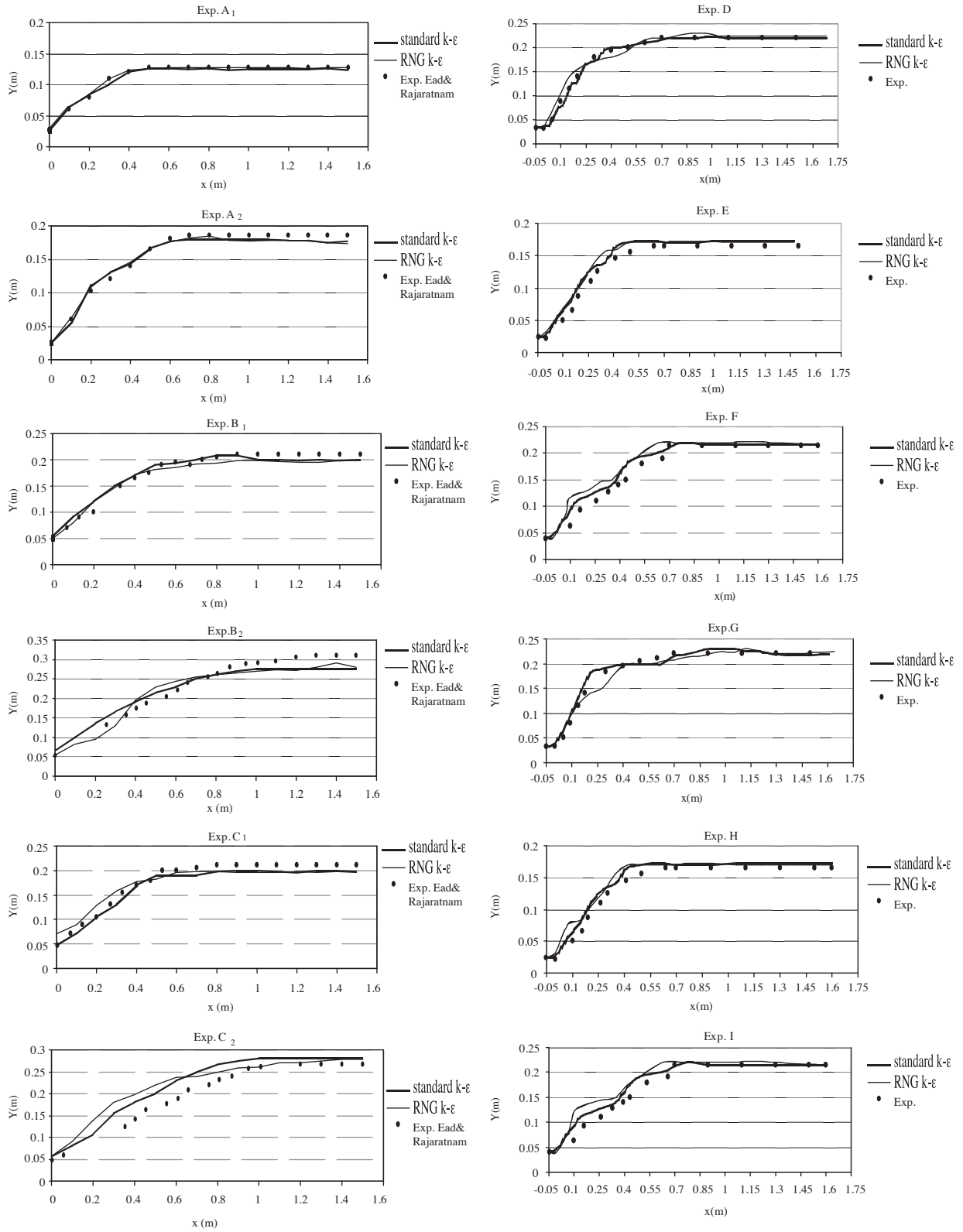
Figure 4. Comparison of free surface profiles between numerical turbulent models and the experimental data.

Also to find similarity of the velocity profiles in the forward flow, variation of the maximum velocity and the length scale, namely u_m and b, with the longitudinal distance was studied. The initial velocity in the supercritical stream just before the jump u_1, was in the range of 2.5–4.07 m/s and the maximum velocity at the last section of measurement was in the range of 0.8–1.5 m/s.

Figure 7 shows the variation of length scale b/y_1 with the normalized longitudinal distance x/y_1. The linear relationship between b/y_1 and x/y_1 for standard k-ε, RNG k-ε models, and experimental data can be described as the following equations respectively:

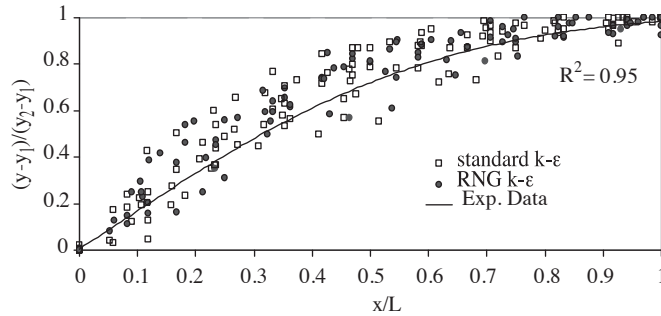$$\left(\frac{b}{y_1}\right)_{sta.} = 0.183\frac{x}{y_1} + 0.88(R^2 = 0.84) \tag{14}$$

Figure 5. Comparison of normalized free surface profiles of jumps on the corrugated bed.
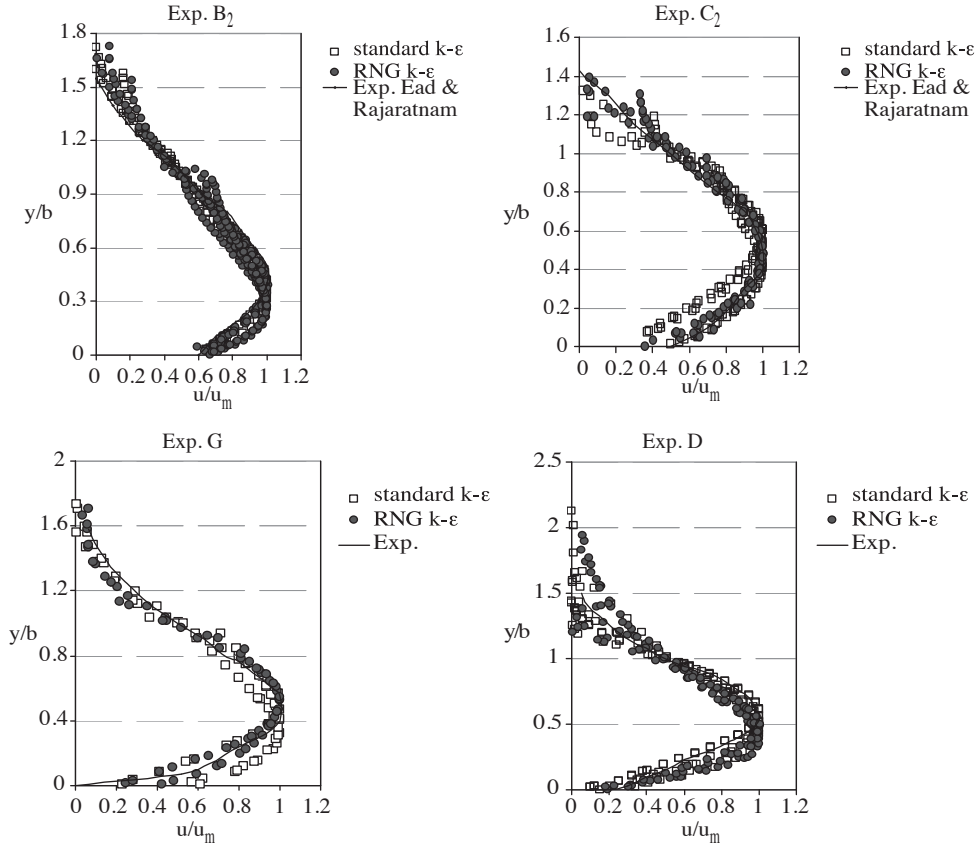

Figure 6. Velocity profiles in the forward flow for experiments B_2 and C_2, D, and G.

$$\left(\frac{b}{y_1}\right)_{RNG} = 0.161\frac{x}{y_1} + 0.87 (R^2 = 0.83) \tag{15}$$

$$\left(\frac{b}{y_1}\right)_{Exp.} = 0.16\frac{x}{y_1} + 0.71 (R^2 = 0.86) \tag{16}$$

A comparison between Eqs. (14) and (15) with Eq. (16) indicates that using the RNG model gives the best agreement with the experimental data.

Figure 8 shows the 2D modeled velocity field at different locations in the hydraulic jump. Figure 8 was also applied to estimate the values of mean velocity in different area of jump.
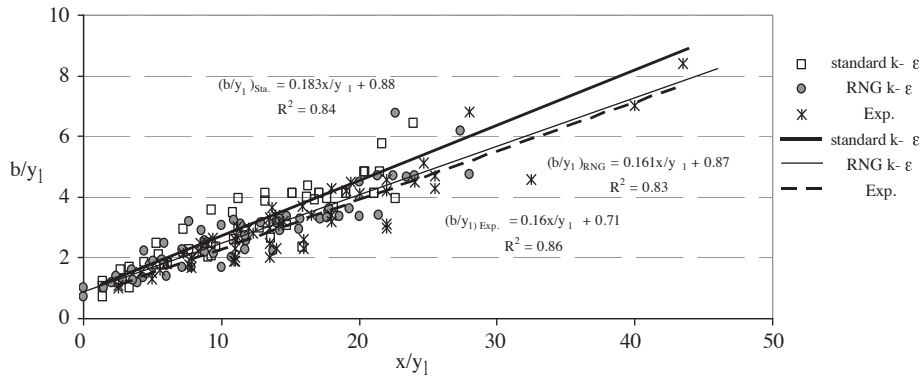

Figure 7. Variation of b/y_1 along longitudinal distance of jump estimated from the turbulent models.
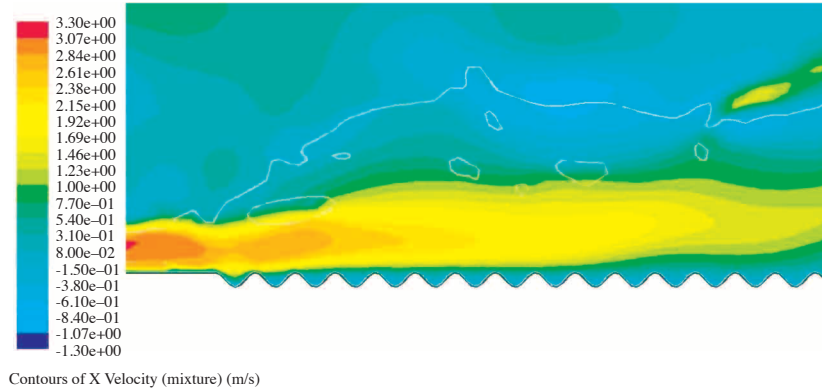

Contours of X Velocity (mixture) (m/s)

Figure 8. Velocity field of the 2D simulation using RNG k-ε model for experiment D.

Bed shear stress

The bed shear stress is obtained using the integral momentum equation. The depth – averaged momentum equation in the longitudinal direction can be derived by integrating Reynolds equation over the depth of flow. The resulting equation can be written as follows:

$$\frac{\partial}{\partial x}\int_o^y \rho u^2 dz + \frac{\partial}{\partial x}\int_0^y p\,dz - \frac{\partial}{\partial x}\int_0^y \sigma_x dz = -\tau_b \tag{17}$$

where ρ = water density; P = hydrostatic pressures; σ_x = Reynolds normal stress; and τ_b = bed shear stress. By using the momentum equation at the sections just before and after the jump, the integrated shear force can be written as follows:

$$F_\tau = \int_{x_1}^{x_2} \tau_b dx = (P_1 - P_2) + M_1 - M_2 \tag{18}$$

where P_1, P_2, M_1, M_2, S_1, and S_2 are integrated pressures, momentum, and normal shear force per unit width at the sections just before and after the jump (Khan and Steffler, 1996).

The shear force coefficient introduced by Wu and Rajaratnam (1995) was defined as:

$$\varepsilon_\tau = \frac{F_\tau}{\gamma y_1^2 / 2} \tag{19}$$

The shear force coefficient ε_τ was obtained by Eqs. (11), (12) and using standard k-ε and RNG k-ε models. In Figure 9, the variation of shear force coefficient ε_τ with Froude number is shown. According to the figure, the experimental results and turbulent models give good estimate of the shear force coefficient ε_τ. The difference between shear force coefficients in both methods is negligible. The equation for the shear stress coefficient may be written as:

$$\varepsilon_\tau = 1.65 Fr_1^2 - 11.25 Fr_1 + 26.2 (R^2 = 0.9) \tag{20}$$
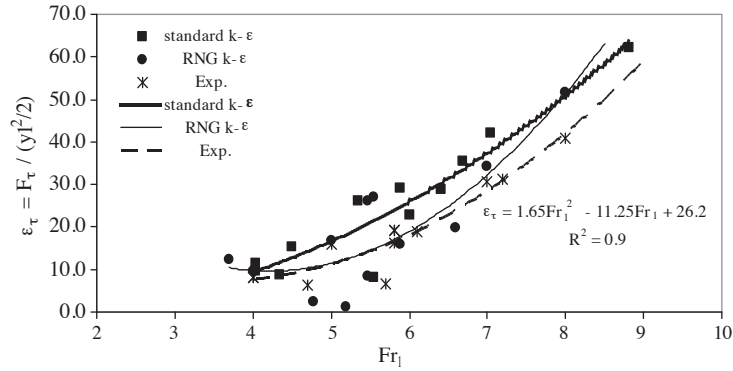
Figure 9. Comparison of shear force coefficient estimated from the turbulent models and the experimental data.
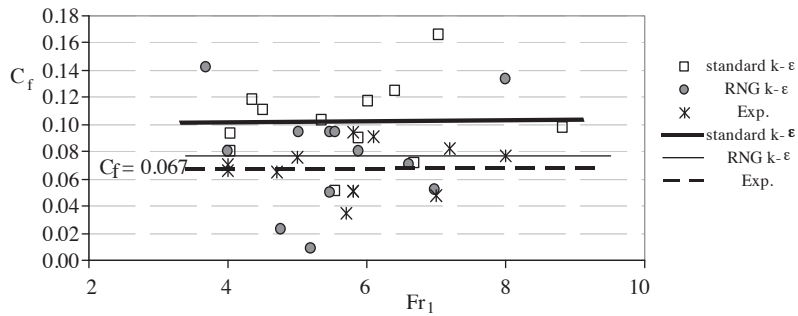
Figure 10. Comparison of coefficient of local skin friction estimated from the turbulent models and the experimental data.

The bed shear stresses were computed using the measured depths just before and after the jump for the standard k-ε and RNG models. The simulated values of bed shear stresses were nearly the same as the

experiment results. The skin friction coefficient can be estimated by the following equation:

$$F_\tau = \int_{X=0}^{L_j} 0.5\rho C_f u_m^2 \Delta x \tag{21}$$

where C_f = coefficient of local skin friction; u_m = maximum velocity at any station, and L_j = length of jump. Figure 10 illustrates the variation of C_f with Froude number, Fr_1. It is seen in the figure that C_f has a mean value of about 0.067 for experimental results and the average values of 0.1 and 0.077 were obtained for standard k-ε and RNG k-ε models, respectively.

Conclusions

The numerical scheme provided by turbulence models was used to predict the 2-D water surface location, flow velocity distribution, and the bed shear stress for jump on a corrugated bed. The computed values were then compared with both the experimental values obtained by Ead and Rajaratnam (2002) and the results of the present study. The computational results showed a close agreement with the various selected experimental results. The water surface profiles can be predicted with an accuracy of 1%-8.6%. The velocity profiles in the boundary layer along the jump are described by the linear relationship between b/y_1 and x/y_1 for standard k-ε, RNG k-ε models, and measured values. It can be seen that the best agreement was obtained between the values calculated from the experimentally measured velocities and RNG model. The momentum equation can be used to obtain a rough estimate of the values of the skin friction. It can be concluded that there is close agreement between the average value of Cf for the experimental values and those obtained using the RNG $k-\varepsilon$ model.

Symbols

b   length scale equal to y where u=0.5u_m and (du/dy) < 0
C_f coefficient of local skin friction
F_τ integrated bed shear force, per unit width, over jump length;
Fr_1 supercritical Froude number=$u_1/(gy_1)^{0.5}$;
g   acceleration due to gravity;
L_j length of jump;
M_1 momentum flux per unit width at the beginning of jump;
M_2 momentum flux per unit width at the end of jump;
P_1 hydrostatic force per unit width at the section just before the jump;
P_2 hydrostatic force per unit width at the section just after the jump;
q   discharge per unit width
Re   Reynolds number= $u_1 y_1 /\upsilon$;
R^2 determination coefficient;
s   wavelength of corrugations;
S_1 normal shear force per unit width at the section just before the jump;
S_2 normal shear force per unit width at the section just after the jump;
S_{ij} mean strain rate;
t   corrugation height;
u_1 depth-averaged velocity at the sections just before the jump;
u_2 depth-averaged velocity at the sections just after the jump;
u   time-averaged longitudinal velocity at any point;
u_m maximum value of u at any station x;

u_i, u_j velocity in i- and j-directions;

x   longitudinal distance measured from section where jump starts;

y   distance from crest of corrugations;

y_1 supercritical initial depth of free jump;

y_2 subcritical depth of jump on corrugated bed;

ε_τ shear force coefficient equal to $F_\tau /gy_1^2/2$;

ε the turbulent dissipation rate

k   the turbulent kinetic energy

μ the viscosity of mixture

μ_A the viscosity of air

μ_t the turbulent (or eddy) viscosity

μ_w the viscosity of water

υ kinematic viscosity of fluid;

ρ mass density of fluid;

τ bed shear stress, also used as suffix.

References

Ead, S.A., Rajaratnam, N. Katopodis, C. and Ade, F., "Turbulent Open-Channel Flow in Circular Corrugated Culverts", J. of Hyd. Eng., ASCE, 126, 750-757, 2000.

Ead, S.A. and Rajaratnam, N., "Hydraulic Jumps on Corrugated Bed", J. of Hyd. Eng., ASCE, 128, 656-663, 2002.

Gharangik, A.M. and Chaudhry, M.H., "Numerical Model of Hydraulic Jump", J. of Hyd. Eng., ASCE, 117, 1195-1209, 1991.

Gonzalez, A. and Bombardelli, F., "Two-Phase Flow Theory and Numerical Models for Hydraulic Jumps, Including Air Entrainment", in Proc. XXXI IAHR Congress, Seoul, Korea, 2005.

Khan, A.A. and Steffler, P.M., "Physically Based Hydraulic Jump Model for Depth-Averaged Computation", J. of Hyd. Eng., ASCE, 122, 540-548, 1996.

Liu, C.R., Ma, W.J. and HuHe, A.D., "Numerical Investigation of Flow Over a Weir", J. of Acta Mechanica Sinica, 18, 594-602, 2002.

Liu, M., Rajaratnam, N. & Zhu, D., "Turbulence Structure of Hydraulic Jumps of Low Froude Numbers", J. of Hyd. Eng., ASCE,130, 511-520, 2004.

Papageorgakis, G.C. and Assanis, D.N., "Comparison of Liner and Nonlinear RNG-Based Models for Incompressible Turbulent Flows", J. of Numerical Heat Transfer, University of Michigan, USA, 35, 1-22 1999.

Sarker, M.A. and Rhodes, D.G., "Physical Modeling and CFD Applied to Hydraulic Jumps", Cranfield University Report, 2002.

Tokyay, N.D., "Effect of Channel Bed Corrugations on Hydraulic Jumps", Impacts of Global Climate Change Conference, EWRI, 15-19 May, Anchorage, Alaska, USA, 2005.

Vischer, D.L. and W.H. Hager, Energy Dissipators, Hydraulic Structures Design Manual, IAHR, A.A. Balkema, Rotterdam, Netherlands, 1995.

Wu S & Rajaratnam N, "Free Jumps, Submerged Jumps and Wall Jets", J. Hyd. Res., 33, 177-212, 1995.

Zhao, Q. and Misra, S.K., "Numerical Study of a Turbulent Hydraulic Jump", Proceeding of 17th Engineering Mechanics Conference, University of Delaware, New York, 2004.